

# Coherent destruction of tunneling in a lattice array with controllable boundary

Liping Li<sup>1</sup>, Xiaobing Luo<sup>2</sup>, Xin-You Lü<sup>1,\*</sup>, Xiaoxue Yang<sup>1</sup>, and Ying Wu<sup>1,†</sup>

<sup>1</sup>Wuhan National Laboratory for Optoelectronics and School of Physics,  
Huazhong University of Science and Technology, Wuhan, 430074, P. R. China and

<sup>2</sup>Department of Physics, Jinggangshan University, Ji'an 343009, P. R. China

(Dated: August 13, 2018)

We have investigated how the dynamics of a quantum particle initially localized in the left boundary site under periodic driving can be manipulated via control of the right boundary site of a lattice array. Because of the adjustable coupling between the right boundary site and its nearest-neighbor, we can realize either coherent destruction of tunneling to coherent tunneling (CDT-CT) transition or coherent tunneling to coherent destruction of tunneling (CT-CDT) transition, by driving the right boundary site while keeping the left boundary site driven by a periodically oscillating field with a fixed driving parameter. In addition, we have also revealed that our proposed CDT-CT transition is robust against the second order coupling (SOC) between next-nearest-neighbor sites in three-site system, whereas localization can be significantly enhanced by SOC in four-site system.

PACS numbers: 42.65.Wi, 42.25.Hz

## I. INTRODUCTION

Coherent control of quantum dynamics via a periodically oscillating external field has been one of the subjects of long-lasting interest in diverse branches of physics and chemistry [1, 2]. One seminal result of the control is coherent destruction of tunneling (CDT), a phenomenon originally discovered by Grossmann *et al.* in 1991 for a periodically driven double-well system [3], upon the occurrence of which the tunneling can be brought to a standstill provided that the system parameters are carefully chosen. Due to its importance for understanding many fundamental time-dependent processes and its potential application in quantum motor [4, 5] and quantum-information processing [6], CDT has received growing attention from both theoretical and experimental studies. Theoretically, it has been extended in various forms such as non-degenerate CDT [7], selective CDT [8], nonlinear CDT [9], many-body CDT [10–13], instantaneous CDT [14] and multiphoton CDT [15]; Experimentally, it has been observed in many different physical systems like modulated optical coupler [16], driven double-well potentials for single-particle tunneling [17], three-dimensional photonic lattices [18], a single electron spin in diamond [19], Bose-Einstein condensates in shaken optical lattices [20, 21], and chaotic microcavity [22].

In addition to conventional approach of modulating a lattice in a uniform fashion, modulating some certain lattice sites selectively also provides an attractive alternative for generation of CDT, in which the rescaled tunneling amplitudes for different sites can be shut off effectively, thereby some intriguing quantum manipulations are realizable such as dissipationless directed transport [23] and beam splitter [24]. CDT was traditionally thought to occur only at the isolated degeneracy point of the quasi-energies and is related to dynamical localization[25]. However, recently a novel quantum phenomenon called dark CDT occurring over a wide range of

system parameters has been introduced in odd- $N$ -state systems [26] which is demonstrated to be caused by localized dark Floquet state that has zero quasi-energy and negligible population at the intermediate state, rather than the superposition of degenerate Floquet states. Those advances on CDT studies offer benefits for coherent control of quantum dynamics.

In this paper, we propose a scheme for the control of quantum tunneling in a periodically driven lattice array with controllable boundary through combination of characteristics of both normal CDT and dark CDT. We consider the coherent motion of a quantum particle in a lattice array, in which the harmonic oscillating external fields act on only the two boundary sites of chain. We have found an interesting result that a single particle initially occupying the left boundary site experiences coherent destruction of tunneling to coherent tunneling (CDT-CT) transition or coherent tunneling to coherent destruction of tunneling (CT-CDT) transition, when the driving amplitude of the external periodic field applied to the right boundary site is increased from zero. We have also revealed that the CDT-CT transition in three-site lattice is robust against the second order coupling (SOC) between next-nearest-neighbor sites, whereas the CT-CDT transition in four-site system is significantly affected by SOC. Moreover, we present a good understanding of the results with help of the high-frequency approximation analysis as well as numerical computation of the corresponding Floquet states and quasi-energies.

## II. MODEL SYSTEM

We consider a single particle in an array of lattice sites with only two boundary sites driven by external periodic field, as shown in Fig. (1). In our model, the left boundary site is driven with fixed driving amplitude and driving frequency, while the right boundary site is driven with varied driving amplitude and fixed driving frequency. In the tight-binding approximation and assuming a coherent dynamics, the single-particle motion can be generally described by the tight-binding Hamiltonian

\*Electronic address: xinyoulu@gmail.com

†Electronic address: yingwu2@126.com

$$\begin{aligned}
H = & E_1(t) |1\rangle \langle 1| + E_N(t) |N\rangle \langle N| + \sum_{j=2}^N \Omega_0 (|j-1\rangle \langle j| + H.c.) \\
& + \sum_{j=2}^{N-1} \nu_0 (|j-1\rangle \langle j+1| + H.c.), \quad (1)
\end{aligned}$$

where  $|j\rangle$  represents the Wannier state localized in the  $j$ th site,  $\Omega_0$  is the coupling strength connecting nearest-neighboring sites, and  $\nu_0$  is the second-order coupling (SOC) strength between next-nearest-neighboring sites. Instead of modulating a lattice in a uniform fashion, we modulate the on-site energies selectively. In this scheme, we assume a harmonic oscillating field applied in form of  $E_1(t) = A_1 \cos(\omega t)$  for site 1, and  $E_N(t) = A_2 \cos(\omega t)$  for site  $N$ . Here  $A_1$  and  $A_2$  are the driving amplitudes and  $\omega$  is the driving frequency, respectively.

We expand the quantum state of system (1) as  $|\psi(t)\rangle = \sum_{j=1}^N a_j(t) |j\rangle$ , where  $a_j(t)$  represents occupation probability amplitudes at the  $j$ th site, with the normalization condition  $\sum_j |a_j(t)|^2 = 1$ . From the Schrödinger equation  $i\partial_t |\psi(t)\rangle = H|\psi(t)\rangle$ , the evolution equation for the probability amplitudes  $a_j(t)$  reads

$$\begin{aligned}
i\frac{da_1}{dt} &= E_1(t) a_1 + \Omega_0 a_2 + \nu_0 a_3 \\
i\frac{da_j}{dt} &= \Omega_0 (a_{j-1} + a_{j+1}) + \nu_0 (a_{j-2} + a_{j+2}) \\
(j = 2, 3, \dots, N-1) \\
i\frac{da_N}{dt} &= E_N(t) a_N + \nu_0 a_{N-2} + \Omega_0 a_{N-1}. \quad (2)
\end{aligned}$$

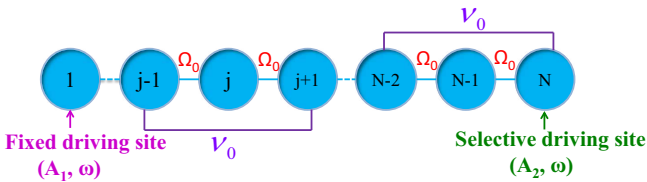


FIG. 1: (Color online) Schematic of a lattice array with controllable boundary for model (1). Here the left boundary site is driven with fixed amplitude  $A_1$  and frequency  $\omega$ , and the right boundary site driven with varied amplitude  $A_2$  and fixed frequency  $\omega$ . All other sites are undriven.

In this work, we mainly illustrate how the quantum dynamics of a single particle initially localized at the left boundary site can be controlled by driving the other boundary site, for both zero and non-zero SOC cases.

### III. CDT CONTROL BY DRIVING THE RIGHT BOUNDARY SITE

#### A. CDT control in three-site system

We start our considerations from the three-site lattice array, the minimal one for odd- $N$ -site system. According to Eq. (2), the evolution equations for the probability amplitudes read,

$$\begin{aligned}
i\frac{da_1}{dt} &= A_1 \cos(\omega t) a_1 + \Omega_0 a_2 + \nu_0 a_3 \\
i\frac{da_2}{dt} &= \Omega_0 a_1 + \Omega_0 a_3 \\
i\frac{da_3}{dt} &= A_2 \cos(\omega t) a_3 + \nu_0 a_1 + \Omega_0 a_2. \quad (3)
\end{aligned}$$

We numerically solve the time-dependent Schrödinger equation (3) with  $\nu_0 = 0$ , i.e., neglecting next-nearest-neighbor tunneling in the chain. The initial state is  $(1, 0, 0)^T$ , and the driving parameters of site 1 fixed as  $A_1 = 22, \omega = 10$ . The evolution of the probability distribution  $P_1 = |a_1|^2$  is presented in figure (2) for three typical driving conditions of site 3. For  $A_2/\omega = 0$ ,  $P_1$  remains near unity, signaling suppression of tunneling. This is the quantum phenomenon well known as CDT. For  $A_2/\omega = 2.0$ ,  $P_1$  oscillates between 1 and  $\sim 0.4$ , showing partial suppression of tunneling. At  $A_2/\omega = 2.4$ ,  $P_1$  oscillates between zero and one, demonstrating no suppression of tunneling. The numerical results clearly indicate that the system undergoes a CDT-CT transition when  $A_2/\omega$  is increased from zero. Such a CDT-CT transition is more clearly demonstrated in Fig. (2)(b), where the minimum value of  $P_1$  is used to measure the suppression of tunneling. When there is large suppression of tunneling,  $\text{Min}(P_1)$  is close to 1; when there is no suppression,  $\text{Min}(P_1)$  is zero. As clearly shown in Fig. (2)(b),  $\text{Min}(P_1)$  slowly falls from its initial value to zero with  $A_2/\omega$  increasing from zero to 2.4. It is observed that the value of  $\text{Min}(P_1)$  drops to zero in narrow intervals around the zeros of  $J_0(A_2/\omega)$ , indicating that the particle is able to tunnel freely from site to site in these regimes.

We explain the above numerical results through some analytic deduction based on high-frequency approximation. In the high-frequency limit, we introduce the transformation  $b_1 = \exp[-i \int A_1 \cos(\omega t) dt] a_1$ ,  $b_2 = a_2$ ,  $b_3 = \exp[-i \int A_2 \cos(\omega t) dt] a_3$ , where  $b_j(t)$  ( $j = 1, 2, 3$ ) are slowly varying functions. Using the expansion  $\exp[\pm i A \sin(\omega t)/\omega] = \sum_k J_k(A/\omega) \exp(\pm i k \omega t)$  in terms of Bessel functions and neglecting all orders except  $k = 0$  in the high frequency region, we arrive at the effective equations of motion,

$$\begin{aligned}
i\frac{db_1}{dt} &= \Omega_0 J_0(A_1/\omega) b_2 \\
i\frac{db_2}{dt} &= \Omega_0 J_0(A_1/\omega) b_1 + \Omega_0 J_0(A_2/\omega) b_3 \\
i\frac{db_3}{dt} &= \Omega_0 J_0(A_2/\omega) b_2. \quad (4)
\end{aligned}$$

Here we have dropped the SOC terms. It is easy to derive the analytical solutions of Eq. (4),

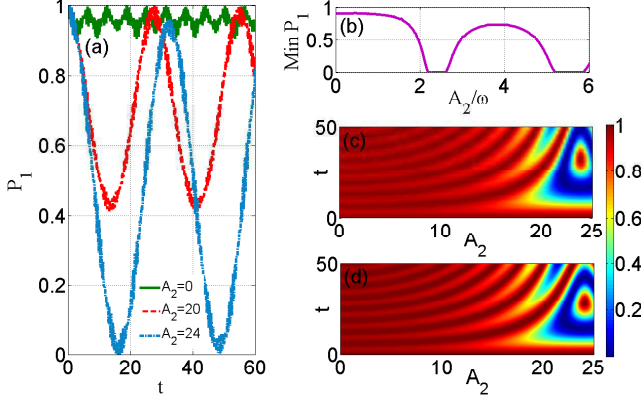


FIG. 2: (Color online) Three-site model (3). (a) Time evolution of the probability at site 1,  $P_1 = |a_1|^2$ , with different values of  $A_2$ ; (b) The minimum value of  $P_1$  as a function of  $A_2/\omega$ ; (c) Numerical results of probability distribution  $P_1$  versus the driving amplitude  $A_2$  and time, obtained from the original model (3); (d) Analytical results of probability distribution  $P_1$  versus the driving amplitude  $A_2$  and time, given by the formula (6). The initial condition is  $\{a_1 = 1, a_2 = 0, a_3 = 0\}$ . The other parameters are chosen as  $A_1 = 22$ ,  $\omega = 10$ ,  $\Omega_0 = 1$ ,  $\nu_0 = 0$ .

$$\begin{aligned} b_1 &= -\frac{J_{02}}{J_{01}}C_1 + i\frac{J_{01}}{\sqrt{J_{01}^2 + J_{02}^2}}[C_2 \sin(Kt) - C_3 \cos(Kt)] \\ b_2 &= C_2 \cos(Kt) + C_3 \sin(Kt) \\ b_3 &= C_1 - i\frac{J_{02}}{\sqrt{J_{01}^2 + J_{02}^2}}[C_2 \sin(Kt) - C_3 \cos(Kt)], \end{aligned} \quad (5)$$

where  $C_j (j = 1, 2, 3)$  are constants to be determined by the initial states and normalization condition,  $J_{01} = J_0 (A_1/\omega)$ ,  $J_{02} = J_0 (A_2/\omega)$  and  $K = \Omega_0 \sqrt{J_{01}^2 + J_{02}^2}$ . Applying the initial conditions  $b_1(0) = 1$ ,  $b_2(0) = 0$ ,  $b_3(0) = 0$  to Eq. (5) yields the undetermined constants  $C_j (j = 1, 2, 3)$  in the forms  $C_1 = -\frac{J_{01}J_{02}}{J_{01}^2 + J_{02}^2}$ ,  $C_2 = 0$ ,  $C_3 = -i\frac{J_{01}}{\sqrt{J_{01}^2 + J_{02}^2}}$  and the occupation probability at site 1 as

$$|b_1|^2 = \left| \frac{J_{02}^2}{J_{01}^2 + J_{02}^2} + \frac{J_{01}^2}{J_{01}^2 + J_{02}^2} \cos(Kt) \right|^2. \quad (6)$$

From expression (6), we immediately have two observations: (i) when  $A_2/\omega \approx 2.4, 5.52$ , i.e., the zeros of  $J_{02}$ , the minimal value of  $|b_1|^2$  is zero; (ii) when  $A_1/\omega$  is tuned near to the zeros of  $J_{01}$  and  $A_2/\omega$  tuned far away from those values,  $|b_1|^2$  remains near unity. The analytical results of  $P_1$  based on formula (6) are plotted in Fig. (2)(d), which agrees well with the numerical results obtained from the original model (3) as shown in Fig. (2)(c).

The Floquet theory provides a powerful tool for understanding the tunneling dynamics obtained in Fig. (2). Since

Hamiltonian (1) is periodic in time,  $H(t + T) = H(t)$ , where  $T = 2\pi/\omega$  is the period of the driving, the Floquet theorem allows us to write solutions of the Schrödinger equation (2) in the form  $a_j(t) = \tilde{a}_j(t) \exp(-i\epsilon t)$ . Here  $\epsilon$  is the quasi-energy, and  $\tilde{a}_j(t)$  is the Floquet state. The Floquet states inherit the period of the Hamiltonian, and are eigenstates of the time evolution operator over one period of the driving

$$U(T, 0) = \mathcal{T} \exp[-i \int_0^T H(t) dt], \quad (7)$$

where  $\mathcal{T}$  is the time-ordering operator. Noticing that eigenvalues of  $U(T, 0)$  are  $\exp(-i\epsilon T)$ , the quasi-energies of this system can be numerically computed by direct diagonalization of  $U(T, 0)$ .

Our numerical results of the quasi-energies and the Floquet states for the modulated three-site system (3) are plotted in Fig. (3). There are three Floquet states with quasi-energies  $\epsilon_1$ ,  $\epsilon_2$  and  $\epsilon_3$ . We immediately notice from Fig. (3)(a) that there exists a dark Floquet state with zero quasi-energy for all of the values of  $A_2/\omega$ . For this three-site system, there is no degeneracy in the quasi-energy levels. Therefore, the occurrence of suppression of tunneling should be further explored through probe into the Floquet states. We display the time-averaged population probability  $\langle P_j \rangle = (\int_0^T dt |a_j|^2)/T$  for a given Floquet state  $(a_1, a_2, a_3)^T$  in Figs. (3)(b)-(d). The Floquet state with  $\langle P_j \rangle > 0.5$  is generally regarded as a state localized at the  $j$ th site. As seen in Figs. (3)(c), the dark Floquet state has negligible population at site 2 while the population  $\langle P_1 \rangle > 0.5$  holds for all values of  $A_2/\omega$  except those in the vicinity of zeros of  $J_0$ . The other two Floquet states are not localized at site 1 since their populations  $\langle P_1 \rangle$  are lower than 0.5. In a word, the CDT-CT transition shown in Fig. (2) comes from the dark Floquet state, whose population  $\langle P_1 \rangle$  undergoes a localization-delocalization transition.

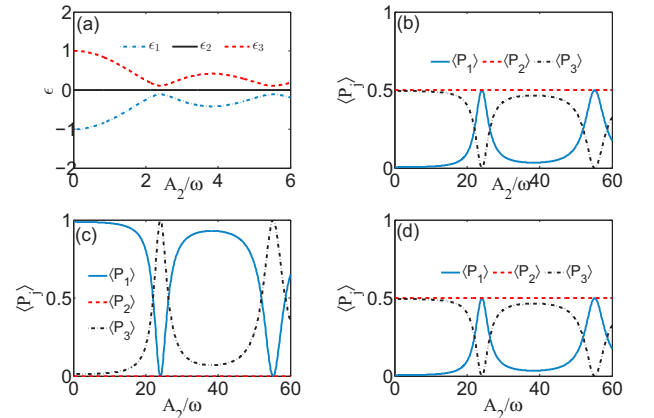


FIG. 3: (Color online) Quasi-energies and Floquet states of three-site system (3). (a) Quasi-energies versus  $A_2/\omega$ . The time-averaged populations for the Floquet state in the quasi-energy level (b)  $\epsilon_1$ , (c)  $\epsilon_2$  and (d)  $\epsilon_3$ . The other parameters are  $\Omega_0 = 1$ ,  $\nu_0 = 0$ ,  $\omega = 10$ .

### B. CDT control in four-site system

We are now in the position to investigate the quantum control of the four-site system. However, similar behaviors discussed in next subsection will appear in six-site lattice system as well. For a four-site system, the coupled equations (2) read,

$$\begin{aligned} i\frac{da_1}{dt} &= A_1 \cos(\omega t)a_1 + \Omega_0 a_2 + \nu_0 a_3 \\ i\frac{da_2}{dt} &= \Omega_0 a_1 + \Omega_0 a_3 + \nu_0 a_4 \\ i\frac{da_3}{dt} &= \nu_0 a_1 + \Omega_0 a_2 + \Omega_0 a_4 \\ i\frac{da_4}{dt} &= A_2 \cos(\omega t)a_4 + \nu_0 a_2 + \Omega_0 a_3. \end{aligned} \quad (8)$$

We plot in Fig. (4)(a) the minimum value of  $P_1$  versus  $A_2/\omega$  by direct numerical simulations of the Schrödinger equation (8) with  $\nu_0 = 0$ . We start a particle at site 1 and fix the driving parameters of site 1 as  $A_1 = 22, \omega = 10$ . As shown in Fig. (4)(a),  $\text{Min}(P_1)$  takes extremely low values about zero except at a series of very sharp peaks. The quasi-energies of this system are shown in Fig. (4)(b), where we find that a pair of quasi-energies cross at the zeros of  $J_0(A_2/\omega)$ . This is the origin of the extremely sharp peaks in localization seen in Fig. (4)(a). Figs. (4)(c)-(f) show that there is no localized Floquet states. These numerical results demonstrate the possibility of inducing CT-CDT transition in four-site system through tuning the rescaled driving amplitude  $A_2/\omega$  from zero to the points of quasi-energy crossing.

### C. Effects of second-order coupling on CDT control

In the above discussion, the influence of second order coupling (SOC), generally thought to be detrimental to CDT, is neglected. In this subsection, We have checked the robustness of our proposed scheme by direct numerical simulations of the Schrödinger equation (2) in the presence of SOC effects. As before, the left boundary site is initially occupied and its driving parameters is fixed as  $A_1 = 22, \omega = 10$ .

The influence of second order coupling on three-site system is plotted in Fig. (5). When SOC effects are taken into account, the numerical results in Figs. (5)(a)-(b) show that the three-site system displays similar dynamical behaviors (CDT-CT transitions) as the case without considering SOC. The numerically computed quasi-energies and Floquet states are depicted in Figs. (5)(c)-(f). Correspondingly, a localization-delocalization transition can be seen for the population distribution  $\langle P_1 \rangle$  of the Floquet state corresponding to a quasi-energy  $\epsilon_2$  close to zero, when  $A_2/\omega$  is increased from zero.

We have also investigated the impact of SOC on the dynamics of four-site system, as shown in Fig. (6). Fig. (6)(a) shows the minimum value of  $P_1$  as a function of the driving amplitude  $A_2/\omega$ . As  $A_2/\omega$  is increased from zero,  $\text{Min}(P_1)$  steadily decreases from a value of  $\sim 0.5$  to zero before it peaks at  $A_2/\omega \approx 2.4$ . Contrary to our expectation, SOC facilitates

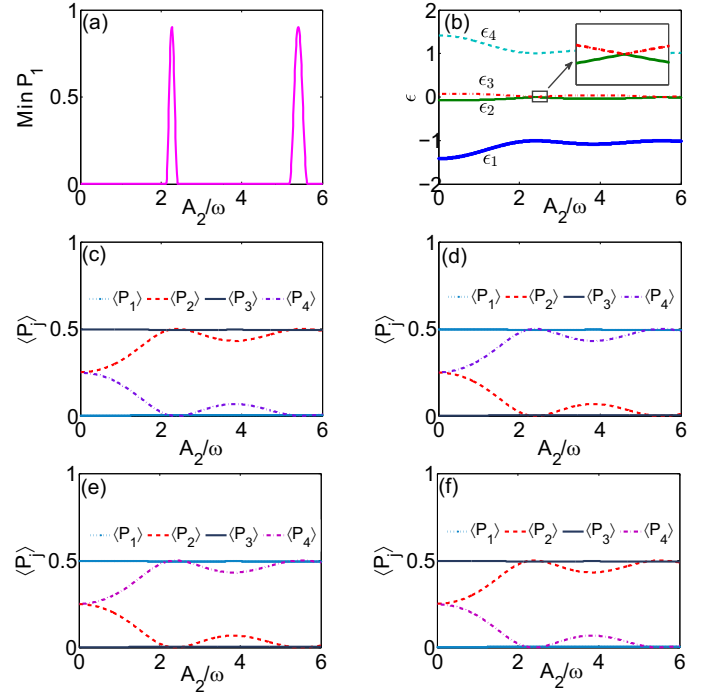


FIG. 4: (Color online) Four-site model described by Eq. (8). (a) The minimum value of  $P_1$  as a function of  $A_2/\omega$ . The extremely narrow peaks appear at the zeros of  $J_0(A_2/\omega)$ . (b) Quasi-energies versus  $A_2/\omega$ . At the zeros of  $J_0(A_2/\omega)$ , a pair of quasi-energies degenerate. (c)-(f) The time-averaged populations  $\langle P_j \rangle$  of the Floquet states corresponding to  $\epsilon_1$ - $\epsilon_4$ . The other parameters are  $A_1 = 22, \omega = 10, \Omega_0 = 1, \nu_0 = 0$ .

rather than hindering the localization. This result is somewhat counter-intuitive. From Fig. (6)(b), it can be seen that a pair of the quasi-energies make a series of close approaches to each other as  $A_2/\omega$  increases. Detailed examination of the close approaches reveals that they are in fact avoided crossings. At the points of close approach, the tunneling is suppressed and the localization peaks. Compared with the zero SOC case shown in Fig. (4), the population distributions of Floquet states change dramatically for four-site system in the presence of SOC effects; see Figs. (6)(c)-(f). The modification of the four-site-system's dynamics due to SOC, such as enhancement of localization, is the consequence of the Floquet states localized at site 1 instead of the quasi-energy degeneracy.

### D. CDT control in five- and six-site systems

Our analysis above is given for three- and four-site systems, but similar behavior can be obtained for other finite number of sites when the SOC effects are not considered.

The quantum dynamics of the driven  $N$ -site systems is investigated by direct integration of the time-dependent Schrödinger equation (2) with the particle initially localized at site 1. In what follows, we will present the numerical re-

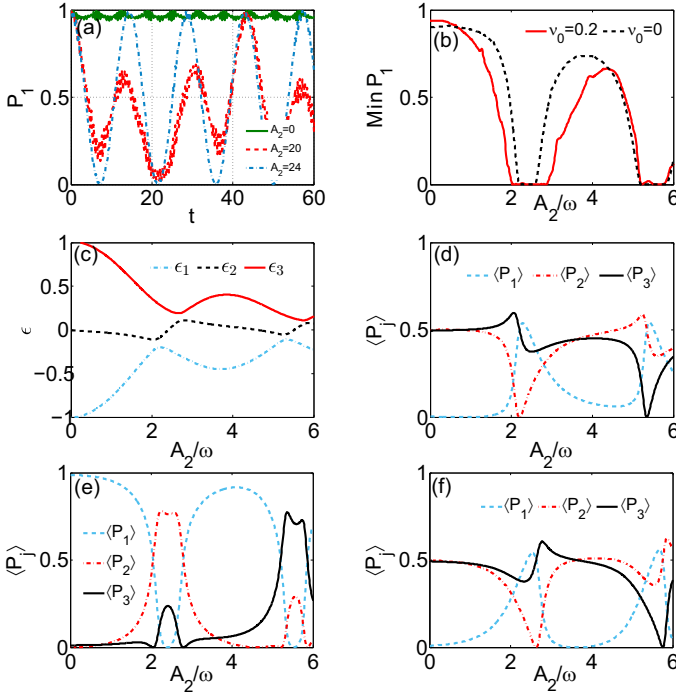


FIG. 5: (Color online) Three-site model (3) with second order coupling. (a) The time evolution of  $P_1$  with different driving amplitude  $A_2$ . (b) The minimum value of  $P_1$  as a function of  $A_2/\omega$ . (c) Quasi-energies versus  $A_2/\omega$ . (d)-(f) The time-averaged populations  $\langle P_j \rangle$  of the Floquet states corresponding to quasi-energies  $\epsilon_1$ - $\epsilon_3$ . The other parameters are  $A_1 = 22$ ,  $\omega = 10$ ,  $\Omega_0 = 1$  and  $v_0 = 0.2$ .

sults for  $N = 5$  and 6. Dynamics for five sites is depicted in Fig. (7), which shows a similar CDT-CT transition as that of three-site system. Like the case of three-site system, this five-site system possesses a dark Floquet state with zero quasi-energy and negligible population at all of the even  $j$ th sites, as illustrated in Figs. (7) (c)-(d). The reason for CDT-CT transition in the five-site system lies in the fact that population distribution  $\langle P_1 \rangle$  for the dark Floquet state also experiences a localization-delocalization transition (see Fig. (7)(d)). When  $N = 6$ , The CDT occurs only at the isolated points of parameters as shown in Fig. (8)(a), where a pair of quasi-energies become degeneracy (Fig. (8)(b)). This is exactly the same as in four-site system. It is demonstrated that the CT-CDT transition can be induced in six-site system by increasing  $A_2/\omega$  from zero.

#### IV. CONCLUSION AND DISCUSSION

In conclusion, we have studied how the dynamics of a single quantum particle initially localized in the left boundary site under periodic driving can be controlled by only driving the right boundary site of a lattice array. In studying the number of lattice sites  $N = 3, 4, 5$  and 6, we have found that (i) a dark Floquet state with a zero quasi-energy exists in the three- and five-site systems. By raising the driving amplitude

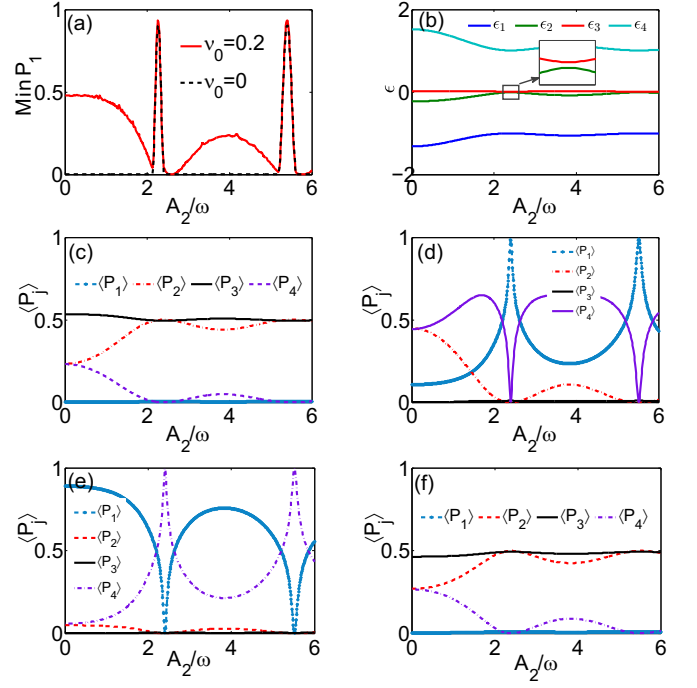


FIG. 6: (Color online) Four-site model (8) with second order coupling. (a) The minimum value of  $P_1$  as a function of  $A_2/\omega$ . (b) Quasi-energies versus  $A_2/\omega$ . (c)-(f) The time-averaged populations  $\langle P_j \rangle$  of the Floquet states corresponding to quasi-energies  $\epsilon_1$ - $\epsilon_4$ . The other parameters are  $A_1 = 22$ ,  $\omega = 10$ ,  $\Omega_0 = 1$  and  $v_0 = 0.2$ .

of the external periodic field applied to the right boundary site from zero, we can induce a CDT-CT transition caused by a localization-delocalization transition of the dark Floquet state; (ii) no localized Floquet state occurs in the four- and six-site systems. However, we can realize a CT-CDT transition in the same way, thanks to the fact that a pair of quasi-energies degenerate at isolate points of parameters. We have also revealed that the CDT-CT transition in three-site lattice persists when the SOC effects are considered. Long-range interactions (non-nearest-neighbor couplings) in the lattice are important and non-negligible in some systems like biomolecules [27], polymer chains [28], coupled waveguides [24], and charge transport in a quantum dot array [29, 30]. Therefore, our proposed scheme provides a new route to possible application of CDT in such systems. Nevertheless, the CT-CDT transition in four-site system is significantly affected by SOC. In such a system, it is found, there exists a counter-intuitive phenomenon that SOC can enhance rather than hinder localization.

Finally, we discuss the experimental possibility of observing our theoretical predictions. The Hamiltonians (1) can be realized in different physical systems, for example using cold atoms or trapped ions in optical lattices [31–33], electron transport in quantum dot chains [30, 34, 35], and light propagation in an array of coupled optical waveguides with harmonic modulation of the refractive index of the selected waveguide along the propagation direction [36, 37]. Recently, several zigzag-type waveguide systems were experimentally realized [38, 39], which provides simpler realization of a one-



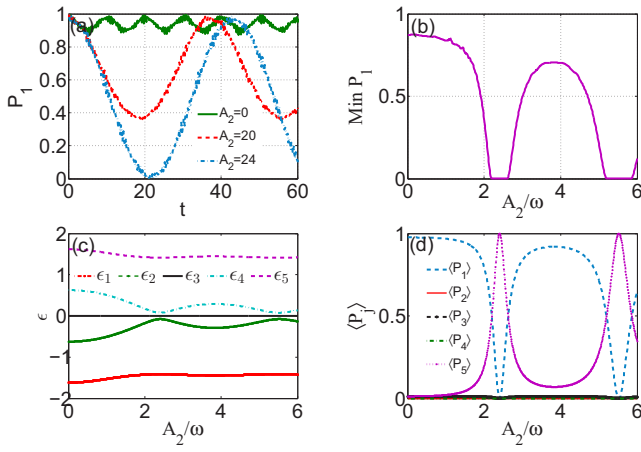


FIG. 7: (Color online) Five-site model. (a) Time evolution of the probability at site 1,  $P_1 = |a_1|^2$ , with different values of  $A_2$ ; (b) The minimum value of  $P_1$  as a function of  $A_2/\omega$ ; (c) Quasi-energies versus  $A_2/\omega$ ; (d) The time-averaged populations  $\langle P_j \rangle$  of the dark Floquet state corresponding to  $\epsilon_3$ . The other parameters are  $A_1 = 22$ ,  $\omega = 10$ ,  $\Omega_0 = 1$ ,  $\nu_0 = 0$ .

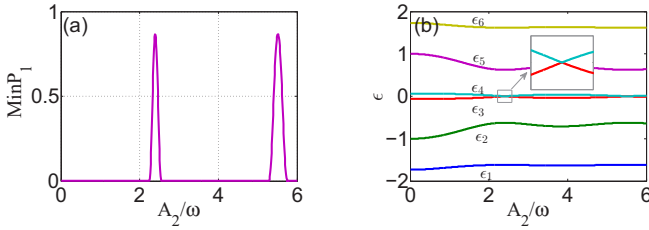


FIG. 8: (Color online) Six-site model. (a) The minimum value of  $P_1$  as a function of  $A_2/\omega$ ; (b) Quasi-energies versus  $A_2/\omega$ . The other parameters are  $A_1 = 22$ ,  $\omega = 10$ ,  $\Omega_0 = 1$ ,  $\nu_0 = 0$ .

dimensional lattice with controllable first- and second-order (that is, next-nearest neighbors) couplings. Though experimental observation of CDT has been reported in many different physical systems, the proofs presented are not so rigorous as claimed, because CDT occurs only at isolated system parameters. Since it is impossible to precisely determine a parameter point through experiment, what is claimed is possibly not a genuine CDT which can be testified only after infinite time of evolution, something unrealizable in real experiment. Due to the limited time of evolution in experiment, the CDT as called may be a pseudo-CDT occurring around the surrounding regime adjacent to an isolated parameter, instead of a real one. Hence, observation of CDT, such as the one in our considered four-site and six-site systems, still present a generally unsolved challenge in current experimental setups

#### Acknowledgments

The work is supported in part by the National Fundamental Research Program of China (Grant No. 2012CB922103), the National Science Foundation (NSF) of China (Grant Nos. 11375067, 11275074, 11374116, 11204096 and 11405061), the Fundamental Research Funds for the Central Universities, HUST (Grant No. 2014QN193). X. Luo is supported by the NSF of China under Grants 11465009, 11165009, 10965001, the Program for New Century Excellent Talents in University of Ministry of Education of China (NCET-13-0836), the financial support from China Scholarship Council, and Scientific and Technological Research Fund of Jiangxi Provincial Education Department under Grant No. GJJ14566. X. Luo also would like to acknowledge his debt to Congjun Wu for providing him with an opportunity of visiting UCSD where part of this work is carried out.

Liping Li and Xiaobing Luo are equally contributed to this work.

- 
- [1] M. Grifoni and P. Hänggi, *Phys. Rep.* **304**, 229 (1998).
  - [2] S.-I. Chu and D. A. Telnov, *Phys. Rep.* **390**, 1 (2004).
  - [3] F. Grossmann, T. Dittrich, P. Jung, and P. Hänggi, *Phys. Rev. Lett.* **67**, 516 (1991); *Z. Phys. B* **84**, 315 (1991).
  - [4] T. Salger, S. Kling, T. King, C. Geckeler, L. M. Molina, and M. Weitz, *Science* **326**, 1241 (2009).
  - [5] G. Lu, W. Hai, *Phys. Rev. A* **83**, 053424 (2011).
  - [6] O. Romero Isart and J. J. García-Ripoll, *Phys. Rev. A* **76**, 052304 (2007).
  - [7] J. T. Stockburger, *Phys. Rev. E* **59**, R4709 (1999).
  - [8] J. M. Villas-Bôas, S. E. Ulloa, and N. Studart, *Phys. Rev. B* **70**, 041302(R) (2004).
  - [9] X. Luo, Q. Xie, and B. Wu, *Phys. Rev. A* **76**, 051802(R) (2007).
  - [10] J. Gong, L. Morales-Molina, and P. Hänggi, *Phys. Rev. Lett.* **103**, 133002 (2009).
  - [11] S. Longhi, *Phys. Rev. A* **86**, 044102 (2012).
  - [12] A. Eckardt, C. Weiss, and M. Holthaus, *Phys. Rev. Lett.* **95**, 260404 (2005).
  - [13] C. E. Creffield and T. S. Monteiro, *Phys. Rev. Lett.* **96**, 210403 (2006).
  - [14] M. Wubs, *Chem. Phys.* **375**, 163 (2010).
  - [15] T.-S. Ho, S.-H. Hung, H.-T. Chen, and S.-I. Chu, *Phys. Rev. B* **79**, 235323 (2009).
  - [16] G. Della Valle, M. Ornigotti, E. Cianci, V. Foglietti, P. Laporta and S. Longhi, *Phys. Rev. Lett.* **98**, 263601 (2007).
  - [17] E. Kierig, U. Schnorrberger, A. Schietinger, J. Tomkovic, and M. K. Oberthaler, *Phys. Rev. Lett.* **100**, 190405 (2008).
  - [18] P. Zhang, N. K. Efremidis, A. Miller, Y. Hu, and Z. Chen, *Opt. Lett.* **35**, 3252 (2010).
  - [19] J. Zhou, P. Huang, Q. Zhang, Z. Wang, T. Tan, X. Xu, F. Shi, X. Rong, S. Ashhab, J. Du, *Phys. Rev. Lett.* **112**, 010503 (2014).
  - [20] H. Lignier, C. Sias, D. Ciampini, Y. Singh, A. Zenesini, O. Morsch, and E. Arimondo, *Phys. Rev. Lett.* **99**, 220403 (2007).
  - [21] A. Eckardt, M. Holthaus, H. Lignier, A. Zenesini, D. Ciampini, O. Morsch, and E. Arimondo, *Phys. Rev. A* **79**, 013611 (2009).
  - [22] Q. Song, Z. Gu, S. Liu and S. Xiao, *Scientific Reports*, **4**, 4858 (2014).
  - [23] J. Gong, D. Poletti, and P. Hänggi, *Phys. Rev. A* **75**, 033602 (2007).
  - [24] X. Luo, J. Huang and C. Lee, *Phys. Rev. A* **84**, 053847 (2011).

- [25] D. H. Dunlap and V. M. Kenkre, Phys. Rev. B **34**, 3625 (1986).
- [26] X. Luo, L. Li, L. You and B. Wu. New J. Phys. **16**, 013007 (2014).
- [27] S. Mingaleev, P. Christiansen, Y. Gaididei, M. Johansson and K. Rasmussen, J. Biol. Phys. **25**, 41 (1999).
- [28] D. Hennig, Eur. Phys. J. B **20**, 419 (2001).
- [29] X. G. Zhao, J. Phys. Condens. Matter **6**, 2751 (1994).
- [30] F. R. Braakman, P. Barthelemy, C. Reichl, W. Wegscheider, and L. M. K. Vandersypen, Nature Nanotech. **8**, 432 (2013).
- [31] D. Jaksch and P. Zoller, Ann. Phys. **315**, 52 (2005).
- [32] O. Morsch and M. Oberthaler, Rev. Mod. Phys. **78**, 179 (2006).
- [33] R. Schmied, T. Roscilde, V. Murg, D. Porras, J. I. Cirac, New J. Phys. **10**, 045017 (2008).
- [34] T. Byrnes, N. Y. Kim, K. Kusudo and Y. Yamamoto, Phys. Rev. B **78**, 075320 (2008).
- [35] T. Yamamoto, M. Watanabe, J. Q. You, Yu. A. Pashkin, O. Astafiev, Y. Nakamura, F. Nori, and J. S. Tsai, Phys. Rev. B **77**, 064505 (2008).
- [36] I. L. Garanovich, S. Longhi, A. A. Sukhorukov, and Y. S. Kivshar, Phys. Rep. **518**, 1 (2012).
- [37] S. Longhi, Laser and Photon. Rev. **3**, 243 (2009).
- [38] S. Longhi, F. Dreisow, M. Heinrich, T. Pertsch, A. Tünnermann, S. Nolte and A. Szameit, Phys. Rev. A **82**, 053813 (2010).
- [39] A. Szameit, I. L. Garanovich, M. Heinrich, A. A. Sukhorukov, F. Dreisow, T. Pertsch, S. Nolte, A. Tünnermann, S. Longhi and Y. S. Kivshar, Phys. Rev. Lett. **104**, 223903 (2010).